


A Projection Quality-Driven Tube Current Modulation Method in Cone-Beam CT for IGRT: Proof of Concept

Technology in Cancer Research & Treatment
 2017, Vol. 16(6) 1179–1186
 © The Author(s) 2017
 Reprints and permission:
sagepub.com/journalsPermissions.nav
 DOI: 10.1177/1533034617740283
journals.sagepub.com/home/tct


Kuo Men, PhD¹ and Jianrong Dai, PhD¹

Abstract

Purpose: To develop a projection quality-driven tube current modulation method in cone-beam computed tomography for image-guided radiotherapy based on the prior attenuation information obtained by the planning computed tomography and then evaluate its effect on a reduction in the imaging dose. **Materials and Methods:** The QCKV-I phantom with different thicknesses (0–400 mm) of solid water upon it was used to simulate different attenuation (μ). Projections were acquired with a series of tube current–exposure time product (mAs) settings, and a 2-dimensional contrast to noise ratio was analyzed for each projection to create a lookup table of mAs versus 2-dimensional contrast to noise ratio, μ . Before a patient underwent computed tomography, the maximum attenuation μ_{\max}^0 within the 95% range of each projection angle (θ) was estimated according to the planning computed tomography images. Then, a desired 2-dimensional contrast to noise ratio value was selected, and the mAs setting at θ was calculated with the lookup table of mAs versus 2-dimensional contrast to noise ratio, μ_{\max}^0 . Three-dimensional cone-beam computed tomography images were reconstructed using the projections acquired with the selected mAs. The imaging dose was evaluated with a polymethyl methacrylate dosimetry phantom in terms of volume computed tomography dose index. Image quality was analyzed using a Catphan 503 phantom with an oval body annulus and a pelvis phantom. **Results:** For the Catphan 503 phantom, the cone-beam computed tomography image obtained by the projection quality-driven tube current modulation method had a similar quality to that of conventional cone-beam computed tomography. However, the proposed method could reduce the imaging dose by 16% to 33% to achieve an equivalent contrast to noise ratio value. For the pelvis phantom, the structural similarity index was 0.992 with a dose reduction of 39.7% for the projection quality-driven tube current modulation method. **Conclusions:** The proposed method could reduce the additional dose to the patient while not degrading the image quality for cone-beam computed tomography. The projection quality-driven tube current modulation method could be especially beneficial to patients who undergo cone-beam computed tomography frequently during a treatment course.

Keywords

CBCT, tube current modulation, projection image quality, image-guided radiotherapy, imaging dose

Abbreviations

ATCM, automatic tube current modulation; CBCT, cone-beam computed tomography; CNR, contrast to noise ratio; CTDI, computed tomography dose index; FBCT, fan-beam computed tomography; FOV, field of view; HCR, high-contrast resolution; IGRT, image-guided radiotherapy; LDPE, low-density polyethylene; MTF, modulation transfer function; pCT, planning CT; PQD-TCM, projection quality-driven tube current modulation; PS, polystyrene; 3D, 3-dimensional; ROIs, regions of interest; SPR, scan projection radiograph; 2D, 2-dimensional; SSIM, structural similarity; XVI, X-ray volumetric imaging.

Received: June 26, 2017; Revised: September 28, 2017; Accepted: October 9, 2017.

Introduction

Kilovoltage cone-beam computed tomography (CBCT) installed on linear accelerators can provide detailed volumetric information on patient anatomy at the treatment position. It allows online verification of the 3-dimensional (3D) patient

¹ Department of Radiation Oncology, National Cancer Center/Cancer Hospital, Chinese Academy of Medical Sciences and Peking Union Medical College, Beijing, China

Corresponding Author:

Jianrong Dai, PhD, Department of Radiation Oncology, National Cancer Center/Cancer Hospital, Chinese Academy of Medical Sciences and Peking Union Medical College, Beijing 100021, China.
 Email: dai_jianrong@163.com



Creative Commons Non Commercial CC BY-NC: This article is distributed under the terms of the Creative Commons Attribution-NonCommercial 4.0 License (<http://www.creativecommons.org/licenses/by-nc/4.0/>) which permits non-commercial use, reproduction and distribution of the work without further permission provided the original work is attributed as specified on the SAGE and Open Access pages (<https://us.sagepub.com/en-us/nam/open-access-at-sage>).

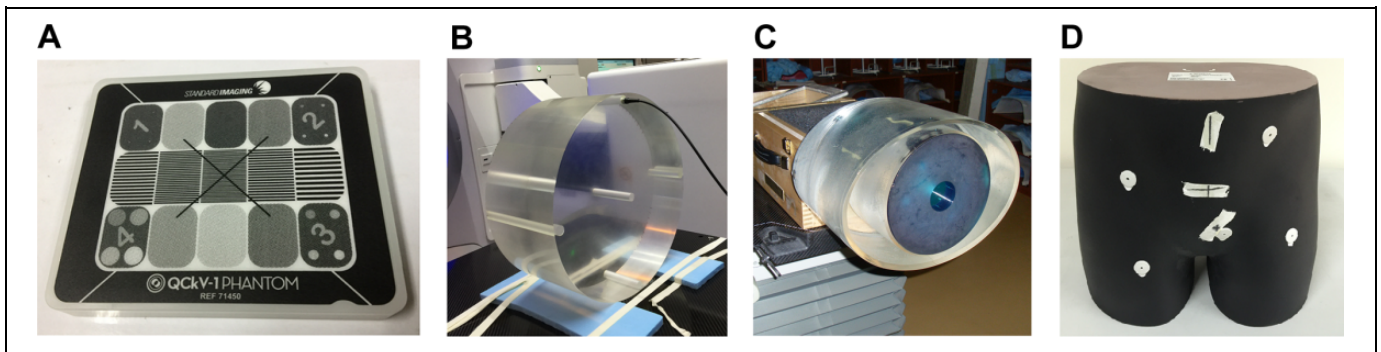


Figure 1. The 4 phantoms: (a) QcKV-1, (b) dosimetry, (c) Catphan 503, and (d) pelvis.

setup for image-guided radiotherapy (IGRT)¹⁻³ and replanning for adaptive radiotherapy.⁴⁻⁶ As a result, CBCT is now used widely to guarantee highly accurate delivery of radiotherapy.

However, repeated use of CBCT in the course of radiotherapy produces a considerable radiation dose to patients,^{7,8} which has aroused growing concern about a potential radiation risk.⁹⁻¹¹ One of the main applicable methods to reduce the dose of CBCT is application of a low tube current–exposure time product (mAs) setting. Some studies^{12,13} have investigated the image quality and imaging dose together as functions of mAs in a qualitative manner to choose the optimal setting. However, a low mAs scheme results in a reduced signal to noise ratio in the projection images due to fewer incident photons interacting with detectors. Accordingly, the reconstructed images are noisy and the image quality degraded. Moreover, if the patient is large (ie, when the X-rays are highly attenuated by an object), there will be streak artifacts due to “photon starvation”¹⁴ at low mAs imaging, whereby the number of detected photons per X-ray is too low.

Cone-beam computed tomography systems for IGRT available in the clinic now adopt a constant mAs setting in a circular scan for a specific site. However, the patient’s anatomy is usually not cylindrical, especially in cases of imaging of the abdomen and/or pelvis. The attenuation of X-rays varies greatly at different scanning angles, which may result in higher mAs than that required in the short-X-ray penetration path or lower mAs in the long-X-ray penetration path. To reduce the patient dose without compromising image quality, automatic tube current modulation (ATCM) has been implemented on commercial systems of fan-beam computed tomography (FBCT).¹⁵⁻¹⁸ The first requirement for the operation of ATCM is the determination of patient attenuation, and this is primarily obtained from the scan projection radiograph (SPR). The methods of ATCM operation are different in CT scanners from different manufacturers. Scanners from Philips (Amsterdam, the Netherlands) and Siemens (Munich, Germany) use the concepts of reference image and reference mAs. However, scanners produced by Toshiba (Tokyo, Japan) and General Electric (Boston, Massachusetts) base the current modulation on a target noise setting. These ATCM systems modulate the X-ray tube current according to the patient’s anatomy along 2 directions. One modulation, named the “longitudinal” or “z”

modulation, is based on different attenuation settings along the longitudinal axis of the patient. The other modulation, called the “angular” or “x-y” modulation, is used to modify the X-ray tube current during rotation around the patient. However, ATCM technology has yet to be applied to CBCT for IGRT.

The aim of the present study was to develop a projection quality-driven tube current modulation (PQD-TCM) method for CBCT. Although noise is the obvious parameter used as the image quality reference, the ability to detect low-contrast tissue in CBCT image depends on the contrast to noise ratio (CNR). Unlike the existing noise-based ATCM methods, we used CNR as the image quality reference to highlight the low-contrast visibility of CBCT. In addition, the patient attenuation could be exactly calculated with the planning CT (pCT) acquired before the use of CBCT, rather than the estimation from SPR. Performance of the proposed method was evaluated in terms of the imaging dose and image quality.

Materials and Methods

Phantoms

Four phantoms available commercially were used in the present study (Figure 1). The QcKV-1 phantom (Standard Imaging, Middleton, Wisconsin) is a dedicated kilovolt X-ray phantom used to analyze the image quality of a 2-dimensional (2D) projection (Figure 1A). It was used to measure and analyze the CNR for 2D projection images (CNR_{2D}). The dosimetry phantom shown in Figure 1B is made of polymethyl methacrylate with a diameter of 32 cm, which meets the specification set by the International Electrotechnical Commission.¹⁹ It was used to measure the computed tomography dose index (CTDI) of CBCT imaging.

Catphan 503 (Phantom Laboratory, Salem, New York) was used to evaluate image quality in a quantitative manner. This phantom is cylindrical with a diameter of 20 cm and a length of 20 cm. To simulate the human body, the Catphan 503 phantom is inserted in an oval body annulus with a major axis of 35 cm and minor axis of 25 cm (Figure 1C).

The pelvis phantom (Phantom Laboratory) consists of soft tissue–equivalent materials and bone–equivalent materials (Figure 1D). Its absorption and scattering properties to

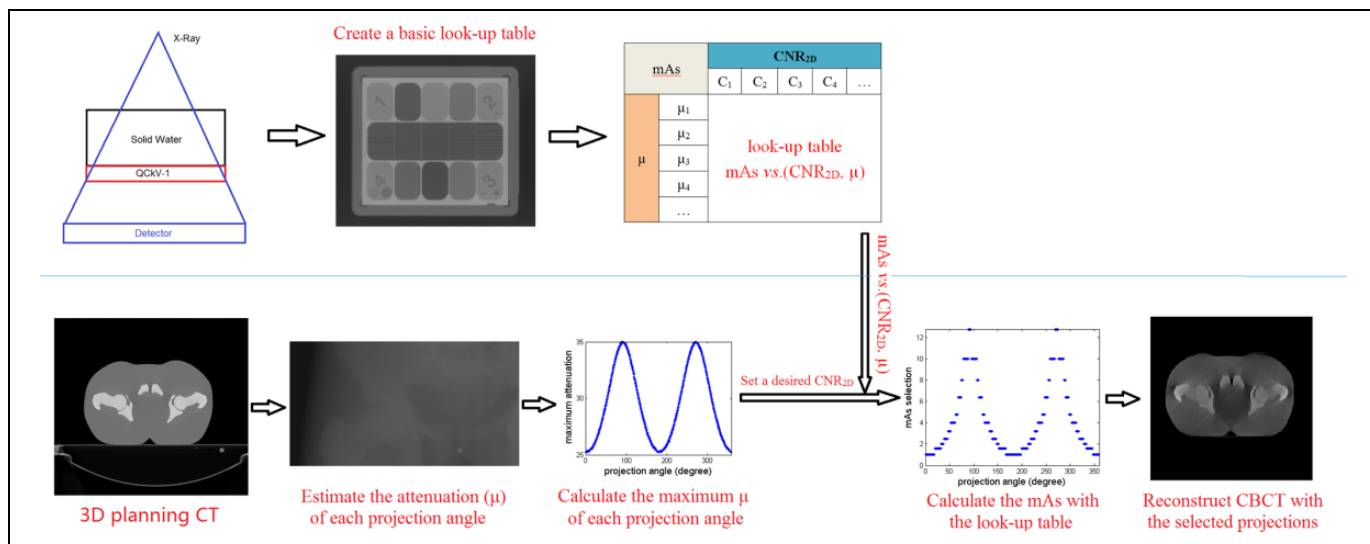


Figure 2. The implementation procedure of the projection quality-driven tube current modulation (PQD-TCM) method.

X-rays are equivalent to those of human tissue. It was used to simulate a noncircular human body.

Cone-Beam Computed Tomography System

Cone-beam computed tomography was done using the X-ray volumetric imaging (XVI) of a Versa HD machine (Elekta, Stockholm, Sweden). The X-ray source uses a rotating anode X-ray tube (D604; Dunlee, Aurora, Illinois) with peak tube potential of 150 kV and maximum current of 500 mA. The detector is an indirect-detection, flat-panel imager with a spatial resolution of 1024 × 1024 arrays of 0.4 × 0.4 mm² pixels (RID1640-A11; PerkinElmer, Waltham, Massachusetts). The source-to-axis distance and source-to-detector distance are 1000 and 1536 mm, respectively. Projections can be acquired with small, medium, and large field of view (FOV). The number of projections for a full 360° rotation is ≈660. X-ray volumetric imaging software uses a cone-beam reconstruction process based on the Feldkamp-Davis-Kress algorithm. A M20 collimator was applied for the body size phantoms. Projections were processed at high resolution to yield projections of dimension 512 × 512 with pixel size of 0.8 × 0.8 mm². Cone-beam computed tomography images were reconstructed with a voxel size of 1.0 × 1.0 × 1.0 mm³.

Projection Quality-Driven Tube Current Modulation Method

For patients with noncylindrical anatomy, the attenuation of X-rays varies greatly at different scanning angles. A higher attenuation in the projection introduces more noise, which degrades the image quality of reconstructed CT. We proposed a PQD-TCM method to modulate the current based on the image quality of the projection.

The implementation procedure of the proposed PQD-TCM method is shown in Figure 2. It had 4 steps, as follows.

Step 1. Create a basic lookup table. The QcKV-1 phantom was placed in the center of the FOV with different thicknesses (0-400 mm) of solid water upon it to simulate different attenuation (μ) values. Projections (p) were acquired with a series of mAs settings, and the CNR_{2D} was analyzed for each projection. Then, a lookup table relating mAs versus CNR_{2D}, μ was created.

Step 2. Estimate the attenuation based on the prior pCT. Patients who underwent radiotherapy usually need to have a CT simulation to acquire their 3D pCT images for treatment planning. In the course of subsequent treatment, CBCT acquired at the treatment position is registered to the pCT for patient’s setup verification. Due to the same setup position of patient in the acquisition of pCT and CBCT, we can have an accurate attenuation (μ) estimation of the patient based on the pCT before CBCT scan. In this step, we first set the treatment center (isocenter) in pCT as the CBCT center. Then the 2D attenuation (μ) maps of each CBCT projection angle (θ) were acquired by projecting the pCT images. Finally, the maximum attenuation μ_{max}^θ within the 95% range of each θ was recorded. It is needed to note that the maximum value was selected within the 95% range of the nonzero μ values (that means ignoring the top 5% of the μ values) to avoid the effects of singular big values.

Step 3. Calculate the mAs with the desired goal. This method allows the user to set a desired CNR_{2D} value, which is used to estimate the tube current. Then, the mAs setting at θ is calculated with the lookup table using mAs versus CNR_{2D}, μ_{max}^θ. Because the mAs setting available in the XVI database is discrete, the closest mAs value is selected for each projection angle.

Step 4. Reconstruct 3D CBCT images using the projections acquired with the selected mAs. The CBCT system available could not change the mAs during a full circular scan. To simulate a series

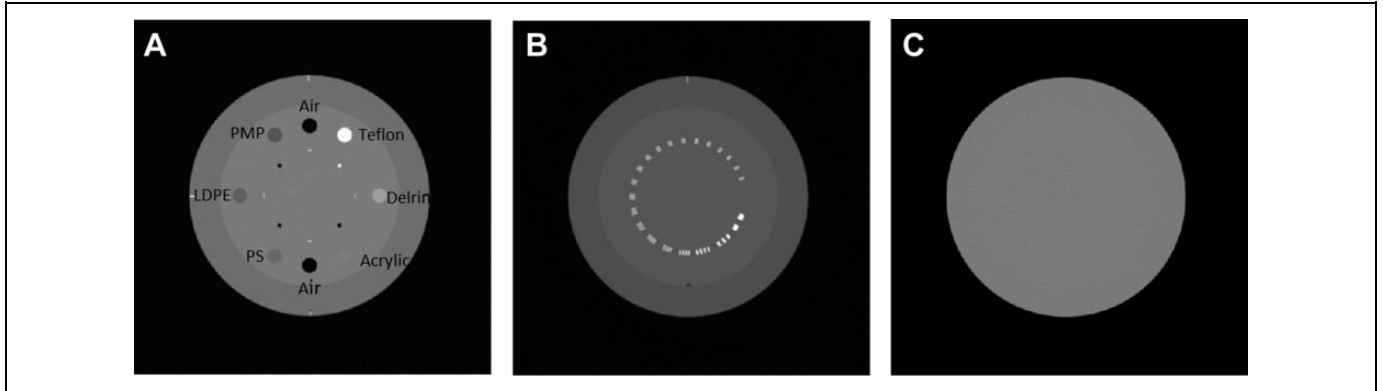


Figure 3. Three modules in Catphan 503 phantom: (A) CTP-404, (B) CTP-528, and (C) CTP-486.

of scans with the selected mAs setting, reconstruction schemes with these projections were achieved by manually selecting the desirable projection frames in the XVI database.

Performance Evaluation

The image quality and imaging dose were measured and analyzed with and without the PQD-TCM method.

Analyses of image quality. The Catphan 503 phantom with the oval body annulus was used to evaluate the image quality in a quantitative manner. The CNR_{2D} values of 0.1, 0.2, 0.3, 0.4, 0.5, 0.6, 0.7, and 0.8 were tested for the PQD-TCM method. Conventional CBCT using a set of constant mAs settings (ie, mAs = 2, 3, 4, 5.12, 6.4, 10, 12.8, and 16 per frame) were also studied for comparison. The indices for the quantitative comparison focused on 3 evaluation metrics including the CNR, the high-contrast resolution (HCR), and the noise level (noise).

Contrast to noise ratio was calculated using the CTP 404 module (Figure 3A). It has 8 embedded rods comprising different materials: air (2 rods), polymethylpentene, low-density polyethylene (LDPE), polystyrene (PS), acrylic, polyoxymethylene (Delrin), and polytetrafluoroethylene (Teflon). Regions of interest (ROIs) of size $4 \times 4 \text{ mm}^2$ within PS and LDPE inserts were used to measure the mean and standard deviation in Hounsfield units. The CNR was calculated using the following equation:

$$CNR = \frac{\text{Mean}_{PS} - \text{Mean}_{LDPE}}{SD_{PS} + SD_{LDPE}} \times 2, \quad (1)$$

where Mean_{PS} and Mean_{LDPE} are the mean voxel values in PS and LDPE, respectively, and SD_{PS} and SD_{LDPE} are the standard deviation in voxel values in PS and LDPE, respectively. Larger CNR value represents higher low-contrast visibility.

High-contrast resolution was measured using the CTP 528 module (Figure 3B and C). It was evaluated with the modulation transfer function (MTF) using a well-known method.²⁰ The evaluation value was 50% of the MTF value ($MTF_{50\%}$) from the MTF curves. Larger $MTF_{50\%}$ value represents better HCR.

Image noise measurements were performed using the CTP 486 module (Figure 3D), which is uniform and water equivalent. The standard deviation (SD) in 5 ROIs of size $10 \times 10 \text{ mm}^2$ (including 1 at the center and 4 at the peripheral positions) was measured. Image noise was calculated as the mean of the 5 SD values.

Image quality was also evaluated using the pelvis phantom. The conventional CBCT used a default mAs setting in the clinic (ie, 16 mAs/frame), whereas the CNR_{2D} value was selected to ensure a maximum mAs of 16 mAs/frame for the PQD-TCM method. The CBCT images obtained by the 2 methods were analyzed using the structural similarity (SSIM) index. The SSIM index is used to measure the similarity between 2 images x and y and is defined as:

$$SSIM(x, y) = \frac{(2m_x m_y + c_1)(2s_{xy} + c_2)}{(m_x^2 + m_y^2 + c_1)(s_x^2 + s_y^2 + c_2)}, \quad (2)$$

where m_x and s_x^2 are the average and variance of x , respectively; m_y and s_y^2 are the average and variance of y , respectively; s_{xy} is the covariance of x and y ; $c_1 = (k_1 L)^2$, $k_1 = 0.01$ and $c_2 = (k_2 L)^2$, $k_2 = 0.03$, L is the dynamic range of the pixel values.

Measurement of imaging dose. For estimation of the radiation exposure of CBCT imaging, the volume CT dose index ($CTDI_{vol}$) was measured. It equals the weighted CT dose index ($CTDI_w$) for CBCT. The center of the dosimetry phantom was placed at the isocenter position of the machine. An ionization chamber (DCT10-RS/Lemo; IBA, Schwarzenbruck, Germany) was used for dose measurements. The dose was measured at 5 positions of the phantom, starting from the phantom center to the 4 peripheral holes. Each measurement was repeated thrice and the average value taken. $CTDI_w$ was calculated from the 5 measurements according to the following formula:

$$CTDI_{vol} = CTDI_w = \frac{CTDI_{center} + 2 \times CTDI_{peripheral}}{3}, \quad (3)$$

where $CTDI_{center}$ is the measured value in the center hole and $CTDI_{peripheral}$ is the average of all 4 peripheral measurements.

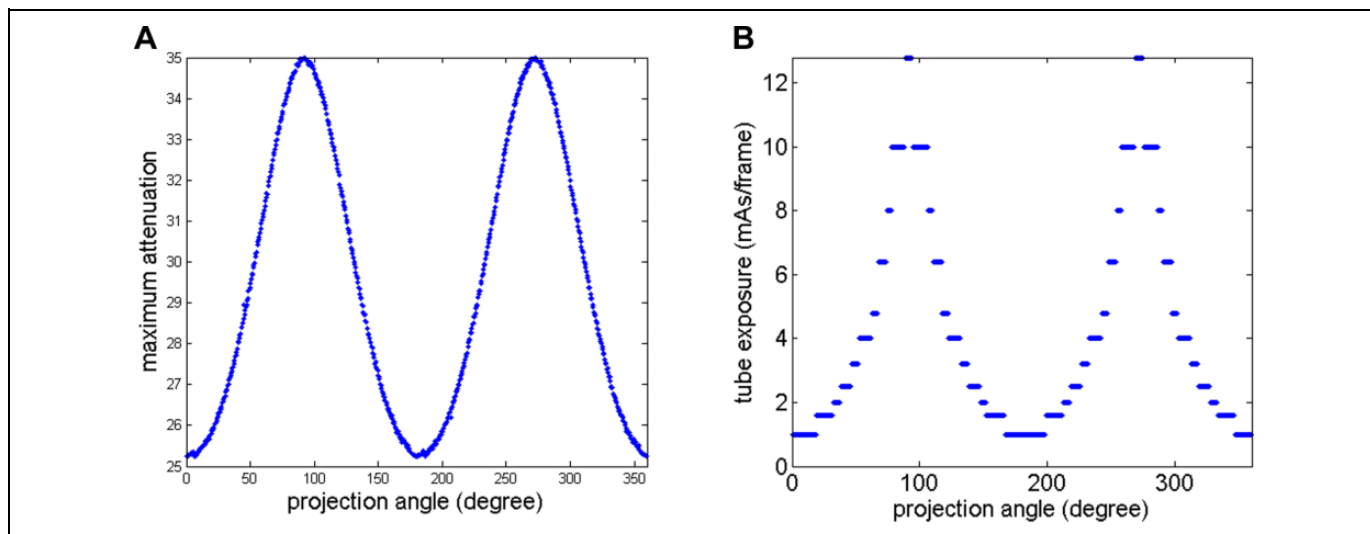


Figure 4. The maximum attenuation (A) and mAs selection for 2-dimensional contrast to noise ratio (CNR_{2D}) = 0.4 (B) of each projection.

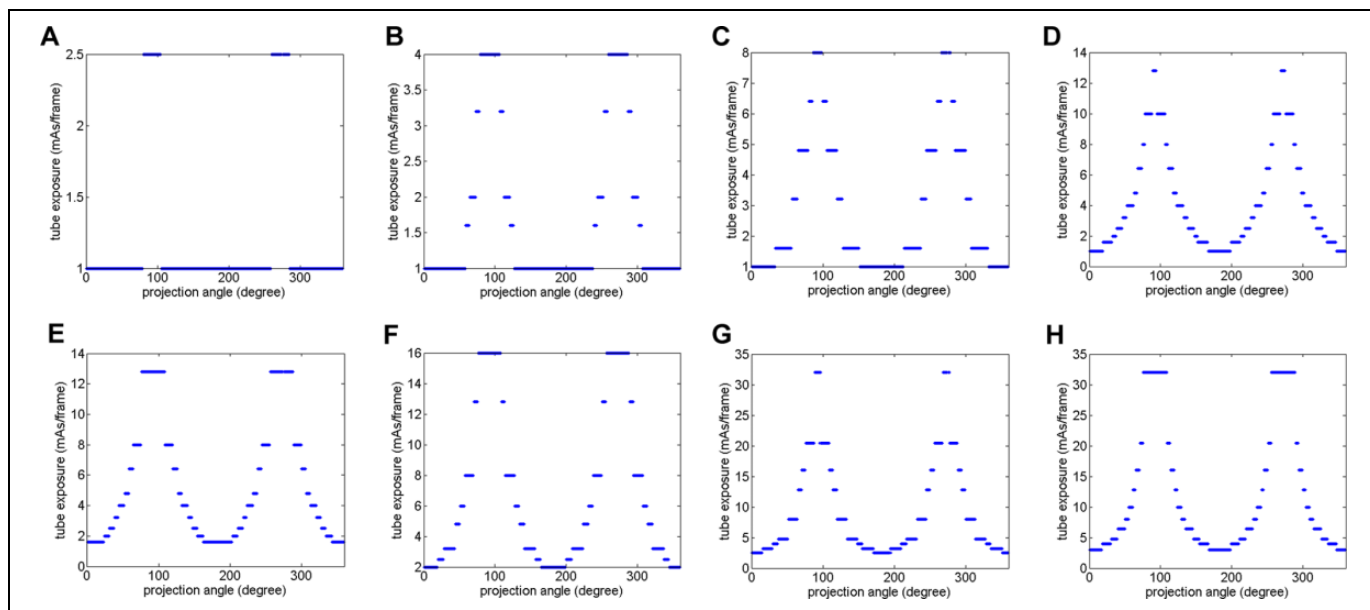


Figure 5. The mAs selection of each projection angle. (A), (B), (C), (D), (E), (F), (G) and (H) are for 2-dimensional contrast to noise ratio (CNR_{2D}) = 0.1, 0.2, 0.3, 0.4, 0.5, 0.6, 0.7, and 0.8, respectively.

Results

Catphan 503

Figure 4A shows maximum attenuation of Catphan 503 phantom of each projection, and Figure 4B shows the corresponding mAs selection for $CNR_{2D} = 0.4$ as an example. According to our method, the higher mAs should be selected at the projection angle with larger attenuation.

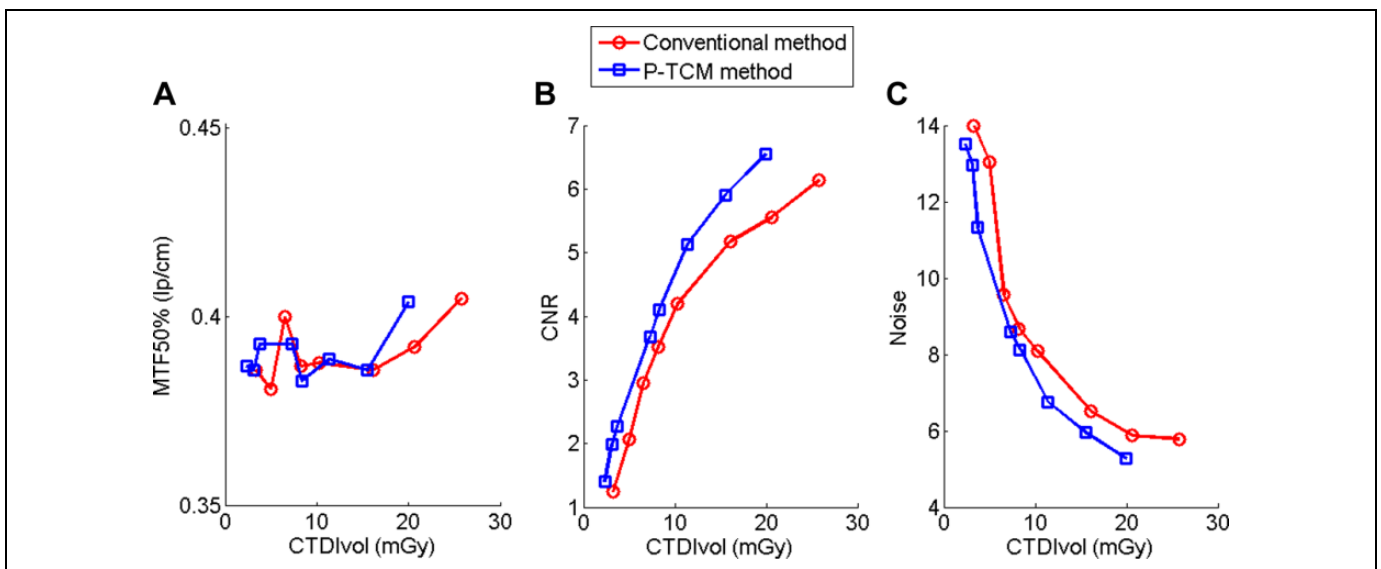
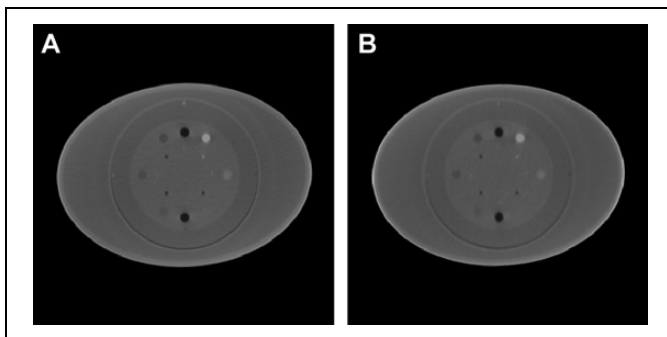
Figure 5 shows the mAs selection of each projection angle for the PQD-TCM method. The selected mAs increased with increases in the desired CNR_{2D} setting. It also varied according to the attenuation of different projection angles at a fixed CNR_{2D} setting. For some projection angles with a short penetrating path, a high mAs was not needed.

The results for the measured $CTDI_{vol}$, $MTF_{50\%}$, CNR, and noise data are listed in Table 1. There was no significant change in the $MTF_{50\%}$ using the 2 methods. However, the PQD-TCM method had a better low-contrast visibility and lower noise than conventional CBCT with the same imaging dose level. The relationship between $CTDI_{vol}$ and image quality is shown in Figure 6 and clearly demonstrates that the PQD-TCM method could reduce the imaging dose by 16% to 33% to achieve a similar image quality to that of conventional CBCT. Figure 7 shows 2 CBCT images acquired with the conventional method and PQD-TCM method, respectively. They had similar CNR values (5.18 and 5.13) and SSIM value (0.999), but the imaging dose was reduced by 29.5%.

Table 1. Results Using the Catphan 503 Phantom.

PQD-TCM	CNR _{2D} = 0.1	CNR _{2D} = 0.2	CNR _{2D} = 0.3	CNR _{2D} = 0.4	CNR _{2D} = 0.5	CNR _{2D} = 0.6	CNR _{2D} = 0.7	CNR _{2D} = 0.8
<i>CTDI_{vol}</i> (mGy)	2.32	3.12	3.73	7.27	8.34	11.38	15.52	19.96
MTF _{50%} (lp/cm)	0.387	0.386	0.393	0.393	0.383	0.389	0.386	0.404
CNR	1.41	1.99	2.27	3.67	4.11	5.13	5.91	6.55
Noise	13.51	12.97	11.32	8.59	8.13	6.76	5.95	5.28
Conventional	mAs = 2	mAs = 3	mAs = 4	mAs = 5.12	mAs = 6.4	mAs = 10	mAs = 12.8	mAs = 16
<i>CTDI_{vol}</i> (mGy)	3.29	5.00	6.54	8.24	10.28	16.13	20.63	25.79
MTF _{50%} (lp/cm)	0.386	0.381	0.400	0.387	0.388	0.386	0.392	0.405
CNR	1.24	2.07	2.95	3.52	4.19	5.18	5.56	6.14
Noise	13.99	13.03	9.56	8.68	8.08	6.51	5.87	5.78

Abbreviations: CNR, contrast to noise ratio; *CTDI_{vol}*, volume CT dose index; MTF, modulation transfer function; MTF_{50%}, 50% of the MTF value; PQD-TCM, projection quality-driven tube current modulation.

**Figure 6.** Image quality as a function of imaging dose: (A) MTF_{50%}; (B) contrast to noise ratio (CNR); (C) noise.**Figure 7.** Cone-beam computed tomography (CBCT) images of Catphan 503: (A) Conventional method; (B) projection quality-driven tube current modulation (PQD-TCM) method.

Pelvis Phantom

The CBCT images for the pelvis phantom are shown in Figure 8. The outline of the phantom was not correct for

conventional CBCT because of photon saturation through the thin edge. The overall SSIM index was 0.992 ± 0.001 for images acquired by the 2 methods. The *CTDI_{vol}* value of the conventional method was 25.79 mGy, but it is reduced by 39.7% using the PQD-TCM method (15.55 mGy).

Discussion

We have designed a PQD-TCM method in CBCT for IGRT. To the best of our knowledge, this task has not previously been reported. We compared the proposed method with the conventional method. This comparison reveals that the CBCT image obtained by the PQD-TCM method had a better low-contrast visibility, lower noise, and similar high-contrast visibility compared with that of conventional CBCT with the same imaging dose level. It could be beneficial to patients who undergo CBCT frequently.

Treatment plans in radiotherapy are designed to deliver a high radiation dose to the tumor target and minimize the

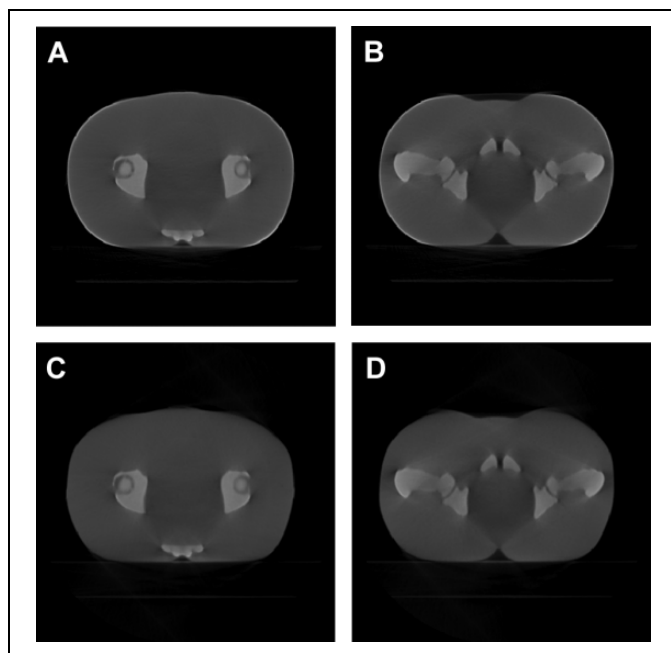


Figure 8. Cone-beam computed tomography (CBCT) images of the pelvis phantom: (A) and (B): Conventional method; (C) and (D): projection quality-driven tube current modulation (PQD-TCM) method.

radiation dose outside the treatment volume. This sharp dose distribution requires accurate positioning of the patient on the treatment couch. To ensure the precision of radiotherapy, CBCT is used frequently for position verification. If we assume that the average prescription dose is 200 cGy per fraction, the percentage dose from CBCT imaging to megavoltage treatment would be $\approx 1\%$ for the body, which is relatively small. However, the “as low as reasonably achievable” principle is always recommended by the radiology community. The strategy presented here shows that there is a potential to reduce the CBCT dose significantly without sacrificing image quality.

Although the ATCM is available in FBCT now, it is different from the proposed PQD-TCM for CBCT in 3 ways. First, CBCT cannot modulate the current in the longitudinal direction because of its cone-shaped beam. Second, the tube current values per rotation are calculated prospectively using an SPR for FBCT, but the proposed method has the advantage of using the prior attenuation information obtained by the pCT. Third, the tube current was selected to achieve the standard or reference noise level for the ATCM systems of FBCT, whereas the PQD-TCM method calculates the tube current based on the CNR of 2D projections.

Tube current modulation technology is not available on current CBCT systems for IGRT, which use a constant current setting during a scan. To combine a group of projections acquired with the desired current at a certain gantry angle, we first scanned the phantoms with a series of current settings to create a database and then extracted the desired projections from the database to reconstruct 3D images. Although for the dose measurement, we measured the imaging dose of the

projections with desired mAs setting separately and then summed them up manually. The methodology described here could aid the design of an imager that would provide tube current modulation technology.

In the present study, the CBCT system of Elekta was used, but it could be applied in other CBCT systems as well. The M20 collimator and F0 filter were tested in the present study as an example. However, analyses of other collimators and filters would be worthwhile to complement the results of the present study in the future. There are some differences between phantoms and human body. The heterogeneity of each person also does exist. Although the experiment results on the 2 phantoms show our method works well, more researches should be carried out before the clinical use.

The scanning FOV is much larger for cone-beam scanning, so it induces more scattering, which is well known to be the most important factor affecting the quality of CBCT images. The experiments demonstrate the proposed method can reduce the imaging dose to patients while not degrading the image quality, although the scatter wasn't corrected. However, scatter may lead to inaccurate dose evaluation. Some researchers have developed different correction strategies. One study²¹ estimated the scatter directly in each projection from pixel values near the edge of the detector behind the collimator leaves. Wu *et al*²² used a novel correction framework to eliminate low-frequency shading artifacts in CT images without relying on prior information. Niu *et al*²³ estimated the primary signals of CBCT projections via forward projection on the pCT image and then obtained the low-frequency errors in CBCT raw projections by subtracting the estimated primary signals and low-pass filtering. Some researchers used effective hardware methods²⁴⁻²⁵ to correct the scatters of kV-CBCT. These effective methods could improve the image quality, and a combination of our method and scattering correction methods merits further investigation.

Conclusion

This work describes a PQD-TCM framework that utilizes the prior information of PCT. The image quality and imaging dose were investigated. We showed that it is possible to reduce the additional dose to a patient while not degrading the image quality. These observations suggest that the proposed method could be applied to the frequently used CBCT in radiotherapy.

Declaration of Conflicting Interests

The author(s) declared no potential conflicts of interest with respect to the research, authorship, and/or publication of this article.

Funding

The author(s) declared the following potential conflicts of interest with respect to the research, authorship, and/or publication of this article: This work was supported by the National Natural Science Foundation of China (grant numbers 11605291;11475261) and the

National Key Projects of Research and Development of China (grant number 2016YFC0904600; 2017YFC0107501).

References

- Létourneau D, Wong JW, Oldham M, et al. Cone-beam-CT guided radiation therapy: technical implementation. *Radiother Oncol.* 2005;75(3):279-286.
- Boda-Heggemann J, Lohr F, Wenz F, et al. kV Cone-beam CT-based IGRT: a clinical review. *Strahlenther Onkol.* 2011;187(5):284-291
- Oldham M, Létourneau D, Watt L, et al. Cone-beam-CT guided radiation therapy: a model for on-line application. *Radiother Oncol.* 2005;75(3):271-278.
- Yadav P, Ramasubramanian V, Paliwal BR. Feasibility study on effect and stability of adaptive radiotherapy on kilovoltage cone beam CT. *Radiol Oncol.* 2011;45(3):220-226.
- Guan H, Dong H. Dose calculation accuracy using cone-beam CT (CBCT) for pelvic adaptive radiotherapy. *Phys Med Biol.* 2009;54(20):6239-6250.
- Ding GX, Duggan DM, Coffey CW, et al. A study on adaptive IMRT treatment planning using kV cone-beam CT. *Radiother Oncol.* 2007;85(1):116-125.
- Alaei P, Spezi E. Imaging dose from cone beam computed tomography in radiation therapy. *Phys Med.* 2015;31(7):647-658.
- Kan M, Leung LW, Lam N. Radiation dose from cone beam computed tomography for image-guided radiation therapy. *Int J Radiat Oncol.* 2008;70(1):272-279.
- Kornerup JS, Brodin NP, Christensen CB, et al. The risk of secondary cancer from paediatric radiotherapy planning PET and CT. Conference: ESTRO, Geneva, Switzerland, 2013.
- Meer AB, Basu PA, Baker LC, et al. Exposure to ionizing radiation and estimate of secondary cancers in the era of high-speed CT scanning: projections from the Medicare population. *J Am Coll Radiol.* 2012;9(4):245-250.
- Dong WK, Chung WK, Ahn SH, et al. Estimate of the secondary cancer risk from megavoltage CT in tomotherapy. *J Korean Phys Soc.* 2013;62(8):1199-1203.
- Sykes JR, Amer A, Czajka J, et al. A feasibility study for image guided radiotherapy using low dose, high speed, cone beam X-ray volumetric imaging. *Radiother Oncol.* 2005;77(1):45-52.
- Yan H, Cervino L, Jia X, et al. A comprehensive study on the relationship between the image quality and imaging dose in low-dose cone beam CT. *Phys Med Biol.* 2012;57(7):2063-2080.
- Mori I, Machida Y, Osanai M, et al. Photon starvation artifacts of X-ray CT: their true cause and a solution. *Radiol Phys Technol.* 2013;6(1):130-141.
- Sookpeng S, Martin C J, Gentle DJ. A study of CT dose distribution in an elliptical phantom and the influence of automatic tube current modulation in the x-y plane. *J Radiol Prot.* 2013;33(2):461-483.
- Sookpeng S, Martin CJ, Gentle DJ. Comparison of different phantom designs for CT scanner automatic tube current modulation system tests. *J Radiol Prot.* 2013;33(4):735-761.
- Moro L, Panizza D, D'Ambrosio D, et al. Considerations on an automatic computed tomography tube current modulation system. *Radiat Prot Dosimetry.* 2013;156(4):525-530.
- Sookpeng S, Martin CJ, Gentle DJ, et al. Relationships between patient size, dose and image noise under automatic tube current modulation systems. *J Radiol Prot.* 2013;34(1):103-123.
- IEC 60601-2-44-2009. *Medical Electrical Equipment—Part 2-44: Particular Requirements for the Basic Safety and Essential Performance of X-ray Equipment for Computed Tomography.* Geneva, Switzerland: The International Electrotechnical Commission (IEC).
- Droege R T, Morin R L. A practical method to measure the MTF of CT scanners. *Med Phys.* 1982;9(5):758-760.
- Siewerdsen JH, Daly MJ, Bakhtiar B, et al. A simple, direct method for x-ray scatter estimation and correction in digital radiography and cone-beam CT. *Med Phys.* 2006;33(1):187-197.
- Wu P, Sun X, Hu H, et al. Iterative CT shading correction with no prior information. *Med Phys.* 2015;42:8437-8455.
- Niu T, Albasheer A, Zhu L. Quantitative cone-beam CT imaging in radiation therapy using planning CT as a prior: first patient studies. *Med Phys.* 2012;39(4):1991-2000.
- Jin JY, Ren L, Liu Q, et al. Combining scatter reduction and correction to improve image quality in cone-beam computed tomography (CBCT). *Med Phys.* 2010;37(11):5634-5644.
- Zhang H, Ren L, Kong V, et al. An interprojection sensor fusion approach to estimate blocked projection signal in synchronized moving grid-based CBCT system. *Med Phys.* 2016;43(1):268-278.